On the Kinetics of Phenol Oxidation in Supercritical Water

Matjaž Krajnc
Laboratory for Catalysis & Chemical Reaction Engineering, The National Institute of Chemistry,
P. O. Box 3430, SI-1001 Ljubljana, Slovenia

Janez Levec
Dept. of Chemical Engineering, University of Ljubljana, P. O. Box 537, SI-1001 Ljubljana, Slovenia

Phenol oxidation in supercritical water was carried out in a tubular laboratory-scale reactor operated at a temperature range of 380°C to 450°C and pressures between 230 and 265 bar. The phenol feed concentrations were between 500 and 1,000 mg/L, while oxygen was fed into the reactor at 50 to 1,000% of the stoichiometric amount needed to oxidize phenol completely to carbon dioxide. Phenol conversions from 16 to 96% were attained as the reactor residence times varied from 15 to 203 s. The oxidation obeys a parallel-consecutive reaction scheme that involves multiring, intermediate products such as phenoxy-phenol, biphenol, dibenzo-dioxin, maleic acid, and succinic acid. Experimental results showed that the phenol disappearance rate is represented well by a power-law kinetic model in which the rate is proportional to the 0.4 power of the oxygen mole fraction and roughly linearly proportional to the phenol mole fraction. The pressure effect on the disappearance rate was appropriately accounted for by introducing the molar volume of the reaction mixture, which was readily calculated by an equation of state. Total organic carbon reduction can be estimated by a lumped kinetic equation. In the P-T region the activation energy of the phenol disappearance was 124.7 kJ/mol.

Introduction

Supercritical water oxidation (SCWO) process takes advantage of the fact that above the critical point of water (374°C and 22.1 MPa), organic compounds as well as oxygen are completely miscible with water. At these conditions, water acts as a fluid with density between that of water vapor and liquid at standard conditions, and exhibits gaslike diffusion rates along with high liquidlike collision rates so that the oxidation takes place in a homogeneous mixture with no mass-transfer limitations. Since the oxidation temperature is much lower than incineration, oxides of nitrogen such as NO and NO_2 are not formed. The high destruction efficiency of supercritical water oxidation has been demonstrated experimentally by Modell and Thomason (1984) in a bench-scale continuous-flow tubular reactor. Various model compounds, including many chlorinated hydrocarbons as well as oxygen- and nitrogen-containing compounds, were efficiently decomposed (over 99.9%).

In comparison with the numerous studies that have been performed in supercritical water, relatively few investigations have been published concerning oxidation kinetics. Some definitive work in determining global rate laws for the oxidation of several simple compounds such as CO, CH_3OH, CH_4, and NH_3 has been reported by Tester's group (Webley and Tester, 1988, 1989; Webley et al., 1990). A review of the kinetic studies in supercritical and subcritical water was given by Li et al. (1991). The thorough work of Thornton and Savage (1990, 1992) on the kinetics of phenol in near-critical and supercritical water ($0.89 \le T_r \le 1.07$ and $0.86 \le P_r \le 1.27$) showed that the reaction was first-order in phenol and half-order in oxygen. Moreover, they found that the reaction was influenced by the overall pressure. They included this pressure effect by introducing water concentration in the rate expression. This approach led to the rate law that was 0.7 order in water. The global kinetics for *o*-chlorophenol disappearance was described by a rate law that was 0.88 order in chlorophenol, 0.41 order in oxygen, and 0.34 order in water

---

Correspondence concerning this article should be addressed to J. Levec.

(Li et al., 1993). The activation energies for the oxidation of phenol and chlorophenol were reported to be 51.9 and 46.0 kJ/mol, respectively. On the other hand, Tufano (1993) claimed that the experimental data of Thornton and Savage (1990) have not been subjected to an adequate kinetic analysis. However, Tufano (1993) reanalyzed the data of Thornton and Savage (1990) by means of a more accurate method and found a surprisingly low value for the activation energy (12.0 ± 7.60 kJ/mol), while the partial orders were found only slightly different, namely, 0.789, 0.46, and 0.52 with respect to phenol, oxygen, and water, respectively.

While supercritical water is a strong solvent for organics, it is a poor solvent for inorganic salts. At around 450°C water loses its ability to dissolve easily soluble inorganic substances. For waste waters containing larger amounts of dissolved inorganic salts it is therefore expected that a commercial SCWO plant would operate in the P-T window defined with $1.01 \le T_r \le 1.12$ and $1.04 \le P_r \le 1.20$. The purpose of this work is, however, to provide kinetic data in the just indicated window for a model pollutant such as phenol, aimed at the development of a rate equation for the SCWO reactor design as well as to examine the existing rate equations. The kinetic data were obtained in an integrally operated, laboratory-scale tubular-flow reactor.

Experimental Studies

Figure 1 is a schematic drawing of the apparatus for supercritical water oxidation used in the present study. The reactor feed streams consisted of aqueous solutions of phenol and hydrogen peroxide, respectively. The feed solutions were maintained oxygen-free by bubbling nitrogen through the feed reservoirs. The solutions were fed into the system by means of high-pressure metering pumps with equal flow rates and preheated separately in a quarter-inch 5-m-long stainless-steel (SS 316) tubing in an oven kept at a constant temperature of 350°C. After passing additional 1.5-m-long preheaters installed in a molten salt bath, the streams were mixed at the reactor entrance, where both attained the desired reaction temperature. In order to ensure immediate and efficient mixing at the reactor entrance, a modified high-resolution mixer developed by Berger et al. (1968) was employed. Its efficiency was tested with a water-dye flow through a mock-up made of plexiglass. A coiled-tube reactor was made of a 6.35-mm-OD (1.59-mm wall thickness) and 5045-mm-long 316 SS tubing. The reactor was centrally placed in the constant-temperature molten salt bath. The molten salt bath was found to be a convenient tool for sustaining isothermal conditions in the reactor due to the high heat capacity of the salt and due to the high reaction heat removal by conduction through the salt. During the operation, the temperature in the reactor was easily kept within ± 1.5°C. The salt composition was selected according to Fox et al. (1988). The temperatures of both feed streams were measured before they entered the preheaters installed in the molten salt bath and in the mixer. Within 1°C the temperature in the mixer was the same as the temperature in the bath for all experiments. The pressure was measured at the pump outlets and at the end of the reactor system. It was maintained within ± 5 bar. At the operating conditions used, the pressure drop through the system was below 5 bar. However, according to the criteria of Cutler et al. (1988), it was assumed that nearly isothermal and isobaric plug flow behavior of the reactor is assured.

The operating conditions used in the experiments are listed in Table 1. A pyrolysis experiment performed in the reactor system at 400°C and 240 bar, and a residence time of 179 s showed that less than 2% of phenol was converted. Hence, the influence of the pyrolytic reactions on the measured oxidation rate is small and can be neglected. As the oxygen source, a 30% aqueous solution of hydrogen peroxide was used. At the operating conditions employed in the preheaters (350°C), the hydrogen peroxide was found to be completely decomposed to oxygen and water. This was concluded from both the negative qualitative test with a mixture of equal parts

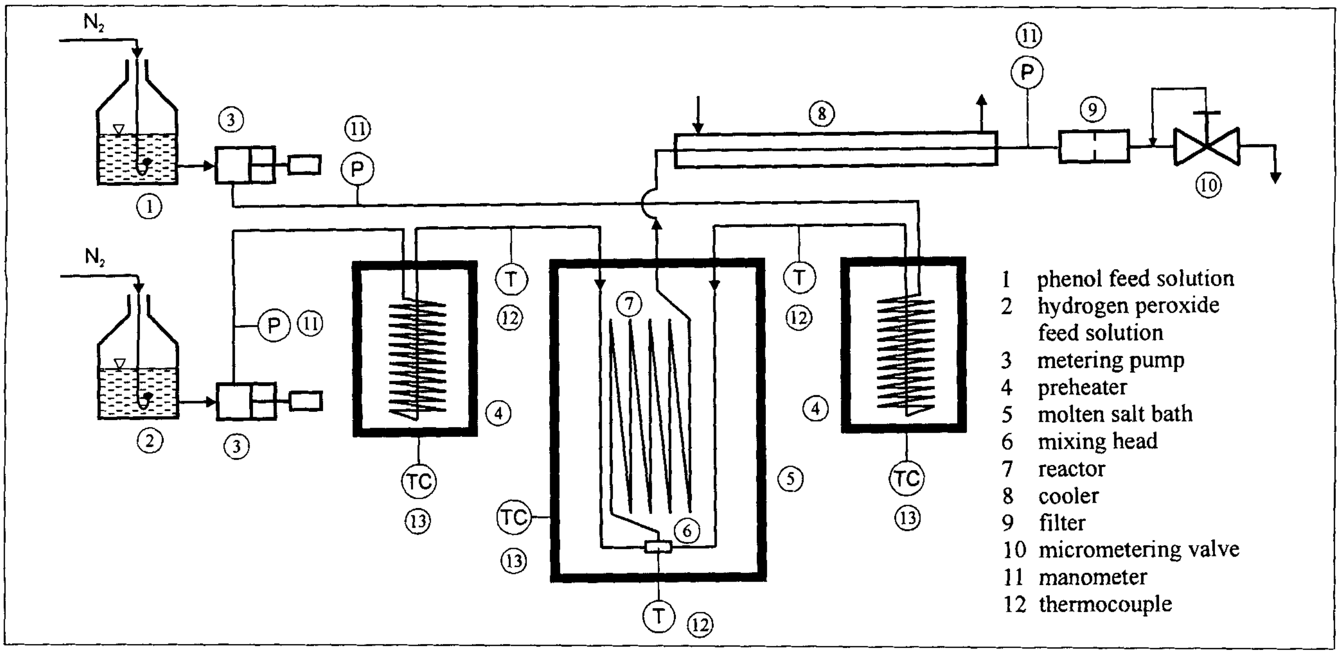

Figure 1. Reactor system.

Table 1. Range of Experimental Conditions

Reactor volume, cm^3	39.95
Liquid flow rate (25°C, 1 bar)	
Phenol feed, cm^3/s	0.0145–0.15
Oxygen feed, cm^3/s	0.0145–0.15
Reactor temperature, °C	380–450
Reactor pressure, bar	230–265
Fluid density in reactor, g/cm^3	0.102–0.372
Fluid viscosity in reactor, Pa·s	2.86×10^{-5}–4.4×10^{-5}
Residence time at operating conditions, s	15–203
Phenol feed concentration, g/L	0.5–1.0
Phenol feed mol fraction	4.68×10^{-5}–9.87×10^{-5}
Oxygen feed concentration, g/L	0.3–12.0
Oxygen feed mol fraction	1.64×10^{-4}–3.33×10^{-3}
Phenol conversion	0.16–0.96

of 0.4% $FeCl_3$ and 0.8% $K_3Fe(CN)_6$ as the reagent, and negative quantitative analysis of the preheater effluent samples by a 0.5-N potassium permanganate solution in the presence of sulfuric acid. The mole ratio of oxygen to phenol varied from 3.5 to 70. In other words, the amount of oxygen fed into the reactor was between 50 and 1,000% of the amount needed stoichiometrically to convert phenol totally to carbon dioxide. The pH value of the reactor effluents was between 3 and 4.

The reactor effluent was cooled in a shell-and-tube-type heat exchanger. After passing through a backpressure regulator (Tescom Model 54-2122W24), the liquid samples were collected and analyzed. Samples were taken after a steady-state operation of the reactor system was reached. The volume of each sample was about three times that of the reactor. Each data point in this work is obtained from the analysis of three samples taken consecutively in 20-min intervals.

The concentration of phenol in the reactor effluent was determined by a high-performance liquid chromatography (HPLC) instrument (TSP constaMetric 350) using Spherisorb ODSR-10 (Phase Separation Ltd.) as a stationary phase, and a mixture of acetonitrile (J.T. Baker) and bidistilled water (volume ratio 1:1) as a mobile phase. A UV spectrophotometer at $\lambda = 270$ nm was employed as a detector. The same instrument was used for the identification of some intermediate products in the reactor effluent. The residual total organic carbon and carbon dioxide concentrations in the samples were measured by means of an advanced DC-190 TOC analyzer (Rosemount/Dohrmann).

The identification of intermediates and products in samples of some representative experiments was performed by means of a Hewlett-Packard GC/MSD system running in both SCAN and SIM modes of operation. A GC (HP 5890A) was equipped with an HP-5 (Ultra-2) high-resolution capillary column (25 m×0.32 mm×0.52 μm), interfaced directly to an HP 5970B quadrupole mass spectrometer as the detector. The chromatographic analysis was optimized to provide the required degree of separation based on the resolution of target compounds. Thus, the GC was operated in the temperature-programming mode with an initial column temperature of 70°C for 2 min, then increased linearly to 250°C at a rate of 10°C, and held at the upper temperature for 10 min. The injector port, equipped with a splitless inlet insert, was set to a temperature of 200°C. The GC/MSD interface was maintained at 260°C. A helium carrier gas of ultrahigh purity was used with a flow rate of 1 mL/min. Before the analysis was performed, solid-phase microextraction was employed to extract analytes from aqueous samples using a SPME syringe assembly (Supelco). Hewlett-Packard ChemStation software was applied to manipulate the gas chromatograph and the mass spectrometer. The latter was tuned daily to validate and monitor its performance. Intermediates and final products were identified by comparing a mass spectrum of a compound with spectra of compounds stored in the NBS library.

Results and Discussion

Reaction pathway

By applying the GC/MSD analysis, the following products were detected in the reactor effluent: dibenzofuran, 2-phenoxy-phenol, 2,2′-biphenol, 4-phenoxy-phenol, dibenzofuranol, and dibenzo-1,4-dioxin, while the HPLC analysis indicated the presence of organic acids propionic, maleic, succinic, formic, and acetic acid. Based on these intermediates/products, the oxidation of phenol in supercritical water may obey a parallel-consecutive reaction scheme such as shown in Figure 2. Indeed, it is very similar to the one proposed by Thornton and Savage (1992b). The intermediate product concentration profiles calculated from the GC/MSD analysis are depicted in Figure 3. The carbon balance was performed for the liquid phase in order to check whether the identified and quantitatively determined intermediates account for all organic carbon that had disappeared. For instance, the phenol concentration at the reactor inlet was 259 mg/L, which corresponds to the carbon inlet concentration of 198 mg/L (at 20°C). The phenol concentration in the reactor outlet was found to be 126 mg/L, that is, 96 mg/L of carbon. In the same effluent we found, by means of a GC/MSD, 44 mg/L of carbon in the form of intermediates listed in Figure 3. Thus, the total carbon in the effluent was equal to 140 mg/L, which yields the carbon conversion of 0.293. On the other hand, total carbon concentration in the reactor effluent was measured by means of a total organic carbon (TOC) instrument. In that case it was found to equal 141 mg/L (20°C). The carbon conversion from this measurement is calculated to be 0.288. These figures are very close, therefore one can conclude that there is no other, unidentified intermediates. At higher residence times (> 100 s) more intermediates were found in the form of highly oxidized compounds (e.g., acids), which were not quantitatively evaluated by means of the GC/MSD analysis. Consequently, the conversions were not as close as in the case of shorter residence times. From the results of Figure 3 one may assume that phenol mainly disappeared via phenoxy-phenols. According to Thornton and Savage (1992b) 4-phenoxy-phenol oxidizes at about three orders of magnitude faster than 2-phenoxy-phenol; therefore, one may further assume that the main phenol oxidation happens via the 4-phenoxy-phenol route. Thornton and Savage (1992b) also reported a relatively low rate of 2,2′-biphenol formation. It should be noted that the late appearance of dibenzofuranol is in agreement with slow biphenol formation and its position in the reaction scheme. The phenol and organic carbon (TOC) concentrations are shown in Figure 4 as a function of residence time for two different oxygen concentrations. As one can see, at a greater excess of oxygen, the difference between the phenol and carbon concentrations—the amount of carbon present in the intermedi-

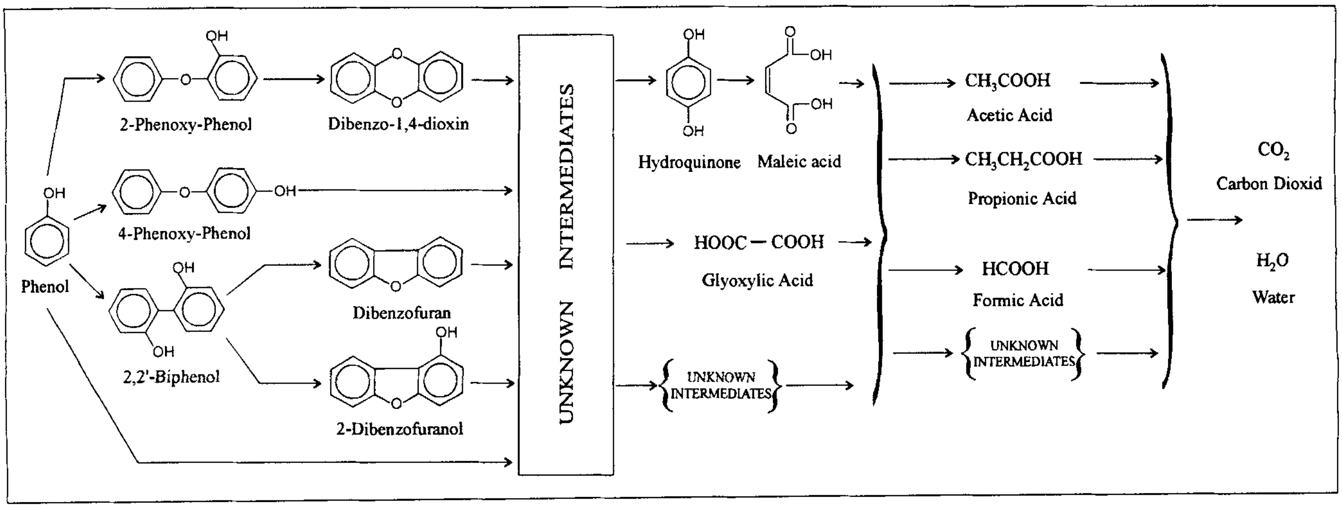

Figure 2. Proposed reaction pathway of phenol oxidation in supercritical water.

ates—remains almost constant, but at a lower oxygen concentration it increases with phenol conversion. These results also suggest that phenol is much more easily oxidized to intermediates than these products. The data in Figure 4 also imply that complete conversion of intermediate products is reached far beyond the phenol conversion. If the stoichiometric amount of oxygen needed to oxidize phenol to carbon dioxide is fed into the reactor, complete oxidation of multiring compounds is unlikely to occur at a reasonable length of a tubular reactor.

At this point it is interesting to compare intermediate products formed during the course of phenol oxidation in supercritical oxidation with those formed during the low-temperature (150°C) catalytic oxidation (Pintar and Levec, 1994). In the latter case only 1,2- and 1,4-benzenedioles, 2,5-cyclohexadiene-1,4-dione, and acetic acid were found as intermediate products. However, these oxygenated compounds are considered more amenable for the oxidation and much less hazardous than those formed in SCWO.

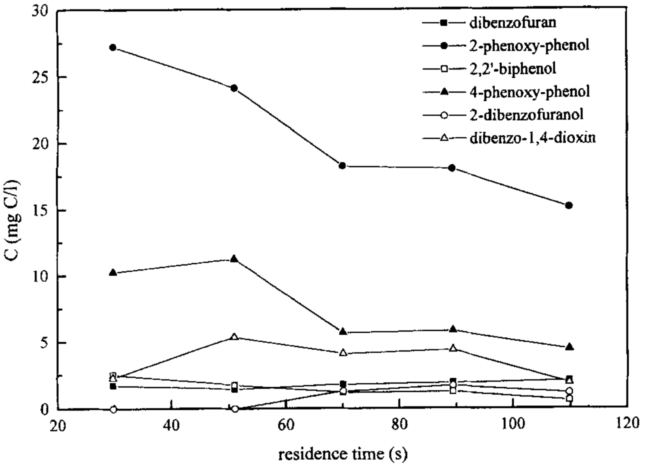

Figure 3. Concentration change of various intermediates during the course of phenol oxidation.

$T = 400°C$, $P = 240$ bar; $n_{O_2}/n_{PhOH} = 70$; $C_{PhOH,feed} = 0.5$ g/L.

Reaction kinetics

Supposing the disappearance rate of a component i in a reaction mixture of components j is given by an overall power-law kinetic model

$$-r_i = k(T)\prod_j C_j^{\alpha_j}; \qquad j = 1,2, \ldots, n, \tag{1}$$

the point mass balance for the component i in an isothermal, isobaric plug-flow reactor is governed by the following equation

$$-\frac{dC_i}{d\bar{t}} = k(T)\prod_j C_j^{\alpha_j}, \tag{2}$$

where the rate constant depends on temperature according to the law proposed by Arrhenius. In the SCWO process, supercritical water is a compressible fluid, therefore the composition-dependent term in Eq. 1 also depends on pressure. In order to avoid the pressure effect, Eq. 2 can be written in

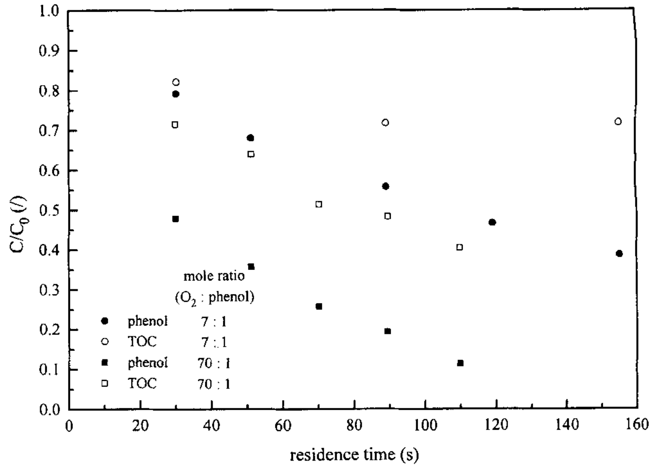

Figure 4. Phenol and TOC concentrations as a function of residence time.

$T = 400°C$; $P = 240$ bar; $C_{PhOH,feed} = 0.5$ g/L.

terms of mole fraction. For that purpose, it is convenient to define the mole fraction as

$$y_i = \frac{C_i}{\sum_j C_j}, \qquad \text{where} \qquad \sum_j C_j = \frac{\sum_j n_j}{V_{\text{mixture}}}. \tag{3}$$

Introducing the molar volume of the reactor mixture

$$V^0 = \frac{V_{mixture}}{\sum_j n_j}, \tag{4}$$

the mole fraction of component i may then be expressed as

$$y_i = C_i \cdot V^0. \tag{5}$$

Combining Eq. 5 and its derivative with Eq. 2 thus gives

$$-\frac{dy_i}{d\bar{t}} = k(T)\left(\frac{1}{V^0}\right)^{\Sigma_j \alpha_j - 1} \prod_j y_j^{\alpha_j}, \tag{6}$$

where the molar volume depends on the temperature and the pressure, as well as on the composition, that is, on the reactor axial coordinate, while the composition-dependent term is temperature and pressure independent. Nevertheless, Eq. 6 can be formally integrated if one assumes the following:

1. The reaction mixture is a very diluted solution of reactants; it consequently leads to

$$\left[\frac{\partial\left(\frac{1}{V^0}\right)}{\partial \bar{t}}\right]_{P,T} = 0$$

2. The high stoichiometric excess of components $j \neq i$ in the reactor feed solution; the concentrations of these components are then independent of the reactor axial coordinate ($dy_{j \neq i}/d\bar{t} = 0$) and are equal to the feed concentrations ($y_{j \neq i} = y_{j \neq i,in}$).

In the case of phenol oxidation in supercritical water reported in this study, the above two conditions were formally fulfilled. Although three components were involved, namely phenol, oxygen, and water, the reactor feed solution always consisted of more than 99% of water. Its impact, if any, on the phenol disappearance rate may therefore be hidden. However, in spite of some evidence in the literature (Thornton and Savage, 1992a) it is assumed that water does not participate appreciably in the oxidation reaction which, on the other hand, is also in agreement with the latest findings of Gopalan and Savage (1994). The phenol disappearance rate can then be written in terms of two components only ($j = 2$), phenol and oxygen, respectively. Equation 6 thus becomes

$$-\frac{dy_{\text{PhOH}}}{d\bar{t}} = k(T)\left(\frac{1}{V^0}\right)^{(a+b)-1} y_{\text{PhOH}}^a y_{\text{O}_2}^b, \tag{7}$$

where a and b are partial orders of the reaction with respect to phenol and oxygen, respectively. An appropriate integration of Eq. 7 yields

$$X_{\text{PhOH}} = 1 - \left[1 - A \exp\left(-\frac{E_a}{RT}\right)\left(\frac{1}{V^0}\right)^{(a+b)-1} (1-a) y_{\text{PhOH},in}^{a-1} y_{\text{O}_2,in}^{b} \bar{t}\right]^{1/(1-a)} \qquad \text{for } a \neq 1, \tag{8}$$

where the local mole fraction of phenol is expressed in terms of its inlet value and the phenol conversion according to

$$X_{\text{PhOH}} = 1 - \frac{y_{\text{PhOH}}}{y_{\text{PhOH},in}}.$$

The objective of the kinetic analysis, however, now is to confront the experimental data obtained in the integral tubular reactor with the integrated rate expression given by Eq. 8. More specifically, the objective is to determine the Arrhenius parameter (A), activation energy (E_a), and reaction orders for phenol (a) and oxygen (b), respectively, from given sets of (X_{PhOH} vs. $\bar{t}$) data. These sets were obtained at various inlet compositions, temperatures, and pressures. Within the critical region of water, the molar volumes at corresponding temperatures and pressures were obtained from the nonclassical scaled equation of state developed by Levelt Sengers et al. (1983), while outside the critical region, it was calculated by using the classic virial equation of state proposed by Haar et al. (1984). The critical region was bounded by a 421.85°C isotherm, 0.20 and 0.42 g/cm^3 isochores, and a segment of vaporization boundary that bridges these isochores. Optimized values of the parameters in Eq. 8 were calculated by means of a multivariable nonlinear regression technique (Marquardt, 1963). The objective function minimized by the regression method was the weighted sum of the squares of the differences between the values of X_{PhOH} calculated from Eq. 8 and those measured experimentally. Confidence intervals of 95% were calculated for the parameters by the regression technique. However, the statistical analysis of all experimentally data points obtained in this study with oxygen-to-phenol molar ratio greater than 7 leads to the final form of Eq. 1:

$$-r_{\text{PhOH}} = (4.903 \pm 0.064)10^8 \exp\left(-\frac{124{,}776 \pm 93}{RT}\right) \times \left(\frac{1}{V^0}\right)^{0.422 \pm 0.005} y_{\text{PhOH}}^{1.041 \pm 0.002} y_{\text{O}_2}^{0.381 \pm 0.003}, \tag{9}$$

which is thought to describe the phenol disappearance rate in supercritical water oxidation. In Eq. 9 E_a and the reaction rate are written in J/mol and mol$_{\text{PhOH}}$/(mol·s), respectively.

The experimental phenol conversions, obtained at five different inlet oxygen concentrations but at a constant temperature and pressure, are shown in Figure 5 as a function of residence time. The proposed kinetic model (Eq. 9) in this figure is represented by solid curves. Good agreement between experimental and predicted values is undeniably achieved except for the runs using 50 and 100% of the stoichiometric amount of oxygen needed to oxidize phenol to

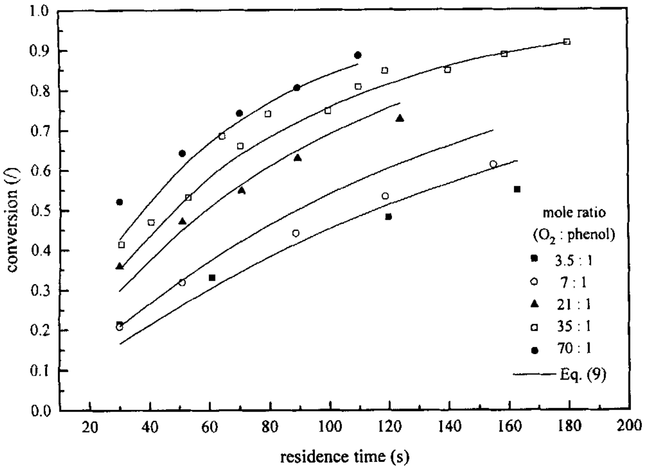

Figure 5. Effect of oxygen concentration on the observed phenol conversion.

$T = 400°C$; $P = 240$ bar; $C_{\mathrm{PhOH,feed}} = 0.5$ g/L.

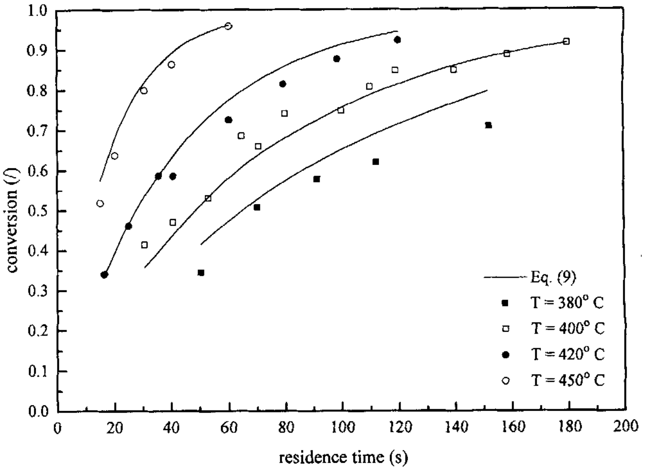

Figure 7. Phenol conversion as a function of residence time at different reaction temperatures.

$P = 240$ bar; $n_{O_2}/n_{\mathrm{PhOH}} = 35$; $C_{\mathrm{PhOH,feed}} = 0.5$ g/L.

carbon dioxide. The disagreement is obvious at higher conversion levels where the lack of oxygen is also caused by its depletion in oxidation of intermediate products. Figure 6 demonstrates the phenol conversion dependence on the inlet phenol concentration. As can be seen, the agreement between predictions of Eq. 9 and experiments is quite good since 300% of the stoichiometric amount of oxygen was used. Figure 7 shows the phenol conversions as a function of residence time at four temperatures in the region between 380 and 450°C. Agreement between predicted and measured values is good again except for the lowest temperature (380°C). However, this temperature is just slightly above the critical temperature where fluid density is very sensitive to pressure oscillation in the system, therefore larger experimental errors of calculated residence time may occur.

The effect of temperature on the reaction rate constant is plotted in Figure 8. Since most of the data were obtained at 400°C, a large scatter at this temperature is expected. The solid line presents a dependence predicted by Eq. 10

$$k = 4.903 \times 10^8 \cdot \exp\left(-\frac{124{,}776}{RT}\right). \tag{10}$$

The activation energy of 124.7 kJ/mol found in this work is higher than the one previously reported by Thornton and Savage (1992a), 51.9 kJ/mol. It should be pointed out that the activation energy in the proposed model is not the intrinsic one. It can be considered as a parameter that predicts the temperature dependence of the phenol disappearance rate in the range investigated. It is also interesting to note that the value reported here is very similar to the one reported by Willms et al. (1987) for wet oxidation. They found the activation energy of 112 kJ/mol in the temperature range between 27 and 227°C.

A parity plot (Figure 9) shows the differences between the phenol conversions calculated by means of Eq. 9 and those measured experimentally in the tubular reactor. As can be seen, the majority of data points are found within a ±10% error band. In other words, 18% of the calculated data points differ more than 10% from their experimental equivalent, and only in 3% of the experiments values exceeded a ±20% er-

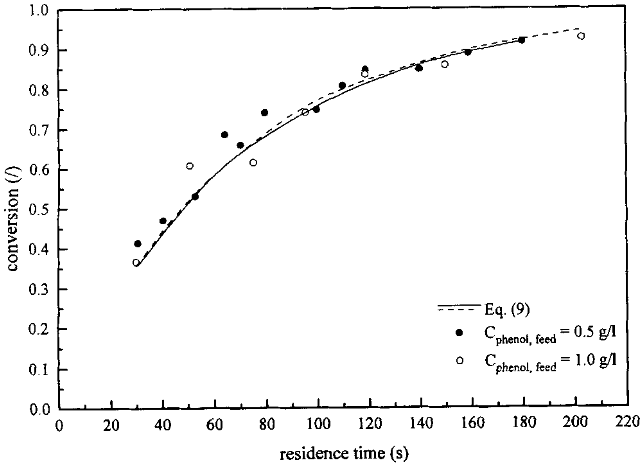

Figure 6. Effect of phenol inlet concentration on the observed phenol conversion.

$T = 400°C$; $P = 240$ bar; $C_{O_2,\mathrm{feed}} = 5.96$ g/L.

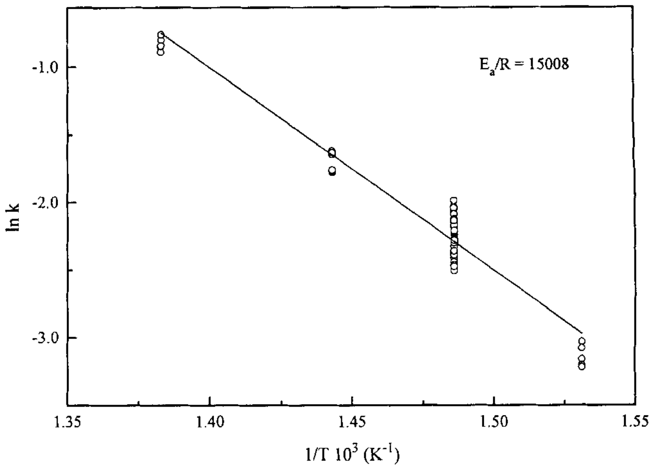

Figure 8. Temperature dependence of the rate constant *k*.

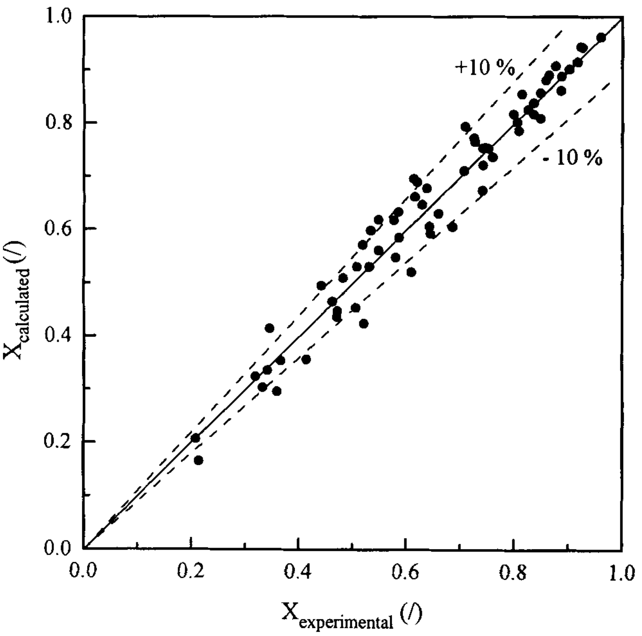

Figure 9. Phenol conversions: experimental measurement vs. Eq. 9 calculation.

ror band. The conversions calculated from the kinetic equation proposed by Thornton and Savage (1992a) are compared in Figure 10 to the experimental conversions obtained in the present work. In this plot many points are located outside the error band. In general, the kinetic equation proposed by Thornton and Savage (1992a) underestimates the phenol conversions at the upper limit of the temperature domain employed in this study (450°C) and overestimates those at the lower limit (380°C). This may be ascribed to the fact that the majority of their experiments (67%) were performed at temperatures around 380°C and only a few (18%) were performed between 400 and 420°C. On the other hand, 380°C is very close to the critical point of water, and due to the high sensitivity of density large experimental errors are possible, as has already been explained. In their analysis data obtained below the critical point were also considered.

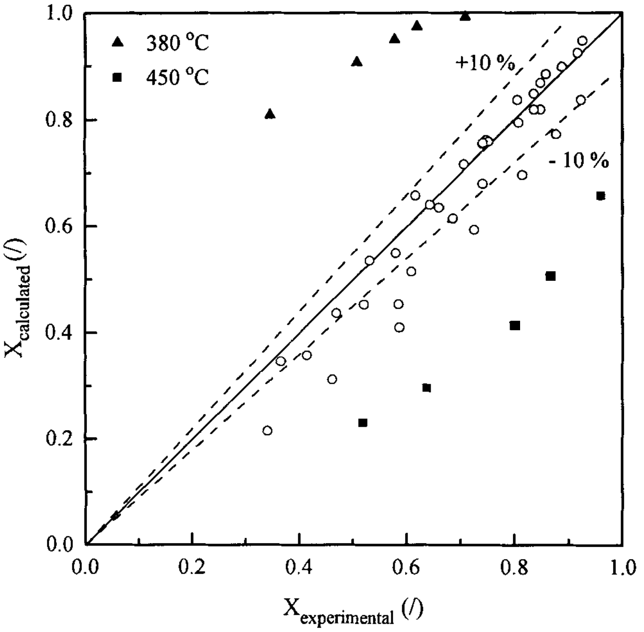

Figure 10. Phenol conversions: experimental measurement vs. Thornton and Savage equation (1992a).

As illustrated in Figure 4, complete oxidation of all intermediate products is accomplished a long time after phenol disappears. It is therefore obvious that the rate equation proposed for the phenol disappearance does not predict the organic carbon conversions, which is the final goal of the SCWO process.

Thus, for the design of an SCWO reactor, a tool capable of predicting complete conversion of all organic species, would be appreciated. An attempt has been made to calculate the TOC disappearance rate from the rate of carbon dioxide evolution (Li et al., 1992). On the other hand, one may look for an equation in the form of Eq. 9, where the phenol conversion is changed for the TOC concentration, that is, the sum of the carbon concentrations of all organic species present in the reaction mixture. However, in this work the experiments were also analyzed with respect to the TOC reduction. The following lumped rate equation for the organic carbon disappearance was obtained by means of the regression analysis

$$-r_{\mathrm{TOC}} = 4.34\cdot 10^{15}\exp\left(-\frac{167{,}831}{R\cdot T}\right)\left(\frac{1}{V^{0}}\right)^{2.03} y_{\mathrm{TOC}}^{2.18}\,y_{\mathrm{O}_2}^{0.85}, \qquad (11)$$

where the E_a is given in J/mol and the rate in $\mathrm{mol_{TOC}}/(\mathrm{mol}\cdot\mathrm{s})$. In the analysis, only experiments with 300 and 1,000% of the stoichiometric amount of oxygen were used due to the fact that only these data may meet the assumption that the oxygen concentration remains constant during the reaction.

Equation 11 can be considered a lumped kinetic equation that seems to describe quite reasonably the behavior of the mixture. By comparing Eq. 11 to Eq. 9, one can conclude that the reaction becomes second-order when the phenol concentration is replaced by the TOC concentration. It is interesting to note that a similar finding has been reported for the cracking of crude oil: in a continuous mixture, essentially a first-order cracking process was best correlated by a second-order reaction when total concentration of the mixture was introduced (Weekman, 1979). However, at this point one may further assume that a theory of lumped kinetics can be a powerful tool for studying oxidation reactions in supercritical water.

A parity plot of the TOC conversions predicted by Eq. 11 and those measured experimentally is depicted in Figure 11. The agreement is excellent for the runs with a high excess of oxygen (300 and 1,000%), but considerably lower when less oxygen is fed into the reactor. This is not surprising since Figure 4 shows that the intermediate products are accumulated in the case of oxygen deficiency. Unfortunately, the length of the tubular reactor employed in this study did not allow us to achieve conversions above 90%. However, the results presented in Figure 11 indicate that an Eq. 11 is capable of predicting the complete TOC reduction.

Conclusions

Phenol oxidation in supercritical water obeys a parallel-consecutive reaction scheme in which multiring species are formed as intermediate products. The results of this investi-

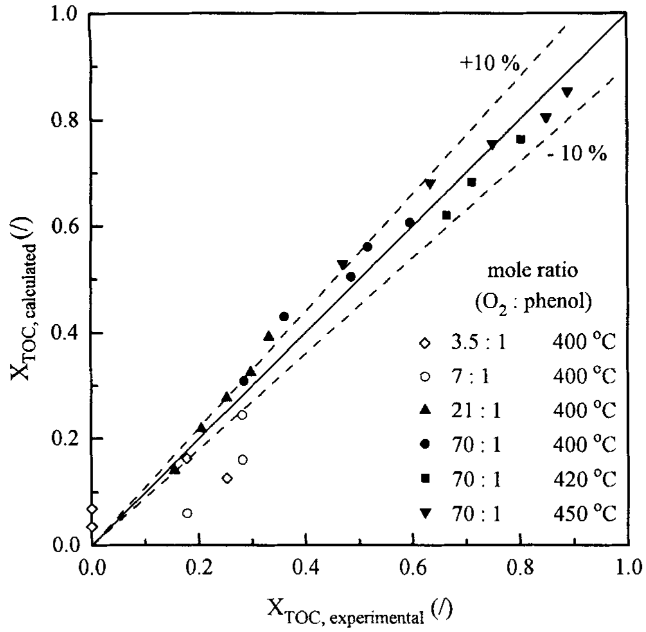

Figure 11. TOC conversions: experimental measurement vs. Eq. 11 calculation.

gation indicate that phenol is much more easily oxidized to intermediates than some of these products up to carbon dioxide. When a high enough excess of oxygen is fed into the reactor, the amount of carbon present in the intermediate products remains constant, but at lower oxygen concentration, this amount increases with phenol conversion. In designing a supercritical oxidation reactor, one should be aware that a complete conversion of intermediate products is reached far beyond the phenol conversion. However, for complete conversion of the organic carbon in a temperature range of 380–450°C, a large excess of oxygen is recommended.

The kinetic equation proposed in this work is, however, obtained in a P-T window that may be used in commercial exploitation of supercritical water oxidation in cases when waste waters contain larger amounts of inorganics. The phenol disappearance rate is found to be well represented by a power-law kinetic model. The rate is proportional to the 0.4 power of oxygen concentration and linearly proportional to the phenol concentration. It seems that the conversion of total organic carbon initially present in the phenol may be effectively predicted by a lumped kinetic equation. The pressure effect on the reaction rate is effectively accounted for by introducing the molar volume of the reaction mixture and by expressing the concentrations in terms of mole fractions.

For design purposes, an equation capable of predicting the total organic carbon conversion is needed. However, some preliminary results of this work suggest that it may be developed for an individual organic species that undergoes oxidation processes or for a mixture of these by using the continuous mixture approach. Future research of oxidation in supercritical water should therefore be directed along these lines.

Acknowledgment

The financial support of this work from the Slovenian Ministry of Science and Technology under grant J2-6179 is gratefully acknowledged.

Notation

C = concentration, mol/L
k = rate constant, $(\text{mol/L})^{1-a-b} \cdot (1/\text{s})$
n = number of moles
P = pressure, bar
P_r = reduced pressure, P/P_{critical}
R = gas constant, J/(mol·K)
r = reaction rate, mol/(L·s)
$\bar{t}$ = residence time, s
T = temperature, K
T_r = reduced temperature, T/T_{critical}
V = volume, L
α = general reaction order

Literature Cited

Berger, R. L., B. Balko, and H. F. Chapman, "High Resolution Mixer for the Study of the Kinetics of Rapid Reactions in Solution," *Rev. Sci. Instrum.*, **39**, 493 (1968).
Cutler, A. H., M. J. Antal, Jr., and M. Jones, Jr., "A Critical Evaluation of the Plug-Flow Idealization of Tubular-Flow Reactor Data," *Ind. Eng. Chem. Res.*, **27**, 691 (1988).
Fox, E., F. Coenen, R. Vermeulen, and G. F. Froment, "A Versatile Bench-Scale Unit for Kinetic Studies of Catalytic Reactions," *Ind. Eng. Chem. Res.*, **27**, 576 (1988).
Gopalan, S., and P. E. Savage, "Reaction Mechanism for Phenol Oxidation in Supercritical Water," *J. Phys. Chem.*, **98**, 12646 (1994).
Haar, L., J. S. Gallagher, and G. S. Kell, *NBS/NRC Steam Tables*, Hemisphere, Washington, DC, p. 320 (1984).
Levelt Sengers, J. M. H., B. Kamgar-Parsi, F. W. Balfour, and J. V. Sengers, "Thermodynamic Properties of Steam in the Critical Region," *J. Phys. Chem. Data.*, **12**, 1 (1983).
Li, L., P. Chen, and E. F. Gloyna, "Generalized Kinetic Model for Wet Oxidation of Organic Compounds," *AIChE J.*, **37**, 1687 (1991).
Li, R., T. D. Thornton, and P. E. Savage, "Kinetics of CO_2 Formation from the Oxidation of Phenols in Supercritical Water," *Environ. Sci. Technol.*, **26**, 2388 (1992).
Li, R. L., P. E. Savage, and D. Szmukler, "2-Chlorophenol Oxidation in Supercritical Water: Global Kinetics and Reaction Products," *AIChE J.*, **39**, 178 (1993).
Marquardt, D. W., "An Algorithm for Least-Squares Estimation of Nonlinear Parameters," *J. Soc. Indust. Appl. Math.*, **11**, 443 (1963).
Modell, M., and T. B. Thomason, "Supercritical Water Destruction of Aqueous Wastes," *Haz. Waste*, **1**, 453 (1984).
Pintar, A., and J. Levec, "Catalytic Liquid-Phase Oxidation of Phenol Aqueous Solutions. A Kinetic Investigation," *Ind. Eng. Chem. Res.*, **33**, 3070 (1994).
Thornton, T. D., and P. E. Savage, "Phenol Oxidation in Supercritical Water," *J. Supercrit. Fluids*, **3**, 240 (1990).
Thornton, T. D., and P. E. Savage, "Kinetics of Phenol Oxidation in Supercritical Water," *AIChE J.*, **38**, 321 (1992a).
Thornton, T. D., and P. E. Savage, "Phenol Oxidation Pathways in Supercritical Water," *Ind. Eng. Chem. Res.*, **31**, 2451 (1992b).
Tufano, V., "A Multi-Step Kinetic Model for Phenol Oxidation in High-Pressure Water," *Chem. Eng. Technol.*, **16**, 186 (1993).
Webley, P. A., and J. W. Tester, "Fundamental Kinetics and Mechanistic Pathways for Oxidation Reactions in Supercritical Water," SAE Tech. Paper Ser. No. 881039, Intersoc. Conf. on Env. Sys., San Francisco (1988).
Webley, P. A., and J. W. Tester, "Fundamental Kinetics of Methanol Oxidation in Supercritical Water," *Supercritical Fluid Science and Technology*, K. P. Johnston and J. M. L. Penninger, eds., ACS Symp. Ser. No. 406, p. 259 (1989).
Webley, P. A., H. R. Holgate, D. M. Stevenson, and J. W. Tester, "Oxidation Kinetics of Model Compounds of Metabolic Waste in Supercritical Water," SAE Tech. Paper Ser. No. 901333, 20th Intersoc. Conf. on Env. Sys., Williamsburg, VI (1990).
Weekman, V. W., "Lumps, Models and Kinetics in Practice," *Chem. Eng. Prog. Monog. Ser.*, **75**, 3 (1979).
Willms, R. S., A. M. Balinsky, D. D. Reible, D. M. Wetzel, and D. P. Harrison, "Aqueous-Phase Oxidation: The Intrinsic Kinetics of Single Organic Compounds," *Ind. Eng. Chem. Res.*, **26**, 148 (1987).

Manuscript received July 24, 1995, and revision received Oct. 30, 1995.